Supplementary material

JunB condensation attenuates vascular endothelial damage under hyperglycemic condition

Xuxia Ren[1,†], Zexu Cui[1,†], Qiaoqiao Zhang[2], Zhiguang Su[3], Wei Xu[1], Jinhui Wu[4,*], and Hao Jiang[1,*]

[1] Laboratory for Aging and Cancer Research, Frontiers Science Center Disease-related Molecular Network, State Key Laboratory of Respiratory Health and Multimorbidity and National Clinical Research Center for Geriatrics, West China Hospital, Sichuan University, Chengdu 610041, China

[2] Key Laboratory of Gene Engineering of the Ministry of Education, State Key Laboratory of Biocontrol, School of Life Sciences, Sun Yat-sen University, Guangzhou 510275, China

[3] Molecular Medicine Research Center, West China Hospital, Sichuan University, Chengdu 610041, China

[4] Center of Geriatrics and Gerontology, National Clinical Research Center for Geriatrics, West China Hospital, Sichuan University, Chengdu 610041, China

[†] These authors contributed equally to this work.

* Correspondence to: Jinhui Wu, E-mail; wujinhui@scu.edu.cn; Hao Jiang, E-mail: haojiang@scu.edu.cn

This PDF file includes:

Supplementary Materials and methods

Supplementary Reference

Supplementary Figures S1–S4

Supplementary Tables S1–S3

Supplementary Materials and methods

Western blotting

Cells grown in 6-well plates were washed twice with PBS, and 100 μl of cell lysis buffer was added to each well. The adherent cells were scraped off with cell scraping on ice and centrifuged at 12000 rpm for 20 min at 4℃. The supernatant was transferred to a new centrifuge tube. To measure the protein concentration, we used the BCA Kit (BOSTER). Protein loading buffer was added to a metal bath at 100℃ for 5 min. Approximately 20 μg of protein per sample was subjected to sodium dodecyl sulfate–polyacrylamide gel electrophoresis (SDS–PAGE) and then transferred to PVDF membranes (Millipore). After sealing with QuickBlock™ Blocking Buffer for Western Blotting (Beyotime) for 1 h, the membranes were incubated with anti-JunB antibody (1:1000, Abcam) or anti-tubulin antibody (1:1000, Cell Signaling Technology). After washing three times with PBST for 10 min, goat anti-rabbit secondary antibodies (1:5000, Thermo) were added and incubated at room temperature for 1 h. After washing three times with PBST for 10 min, ECL Prime Western Blotting Detection Reagent (Thermo) was used to detect chemiluminescent signals.

Coomassie brilliant blue staining

The purified JunB protein was separated by SDS–PAGE and then stained with Coomassie brilliant blue staining solution and 60% perchloric acid. The stained gel was washed with water until the background staining was fully removed.

JunB protein purification

To express and purify His-JunB protein, the plasmid containing His-JunB was transformed into *E. coli* BL21, and a single colony was selected and cultured in 10 ml of LB medium. After 16 h, the colony was poured into 1 L of fresh LB medium and cultured at 37℃ and 220 rpm. When the OD600 reached 0.6–0.8, 1 mM IPTG was added to induce protein expression. The mixture was incubated at 16℃ and 220 rpm for 16 h and centrifuged at 4℃, 3800 rpm to collect bacteria. Then, lysis buffer (50 mM NaH_2PO_4, 300 mM NaCl, 10 mM imidazole, 1 mM PMSF, pH 8) was added to the bacteria, followed by ultrasonic lysis for 15 min, and the supernatant was collected at 4℃, 12000 rpm. The supernatants were added to the columns with Ni-NTA beads (Qiagen). After slowly rotating for 4 h, the unbound proteins were washed with wash buffer (50 mM NaH_2PO_4, 300 mM NaCl, 20 mM imidazole, pH 8). Finally, elution buffer (50 mM NaH_2PO_4, 300 mM NaCl, 500 mM imidazole, pH 8) was used to elute the protein. The protein collected in elution was concentrated by an Amicon Ultra 30K device (Millipore). At the same time, frozen fresh PBS was added, and the process was repeated three times to a volume of 200–500 μl. The purified protein was quantified using an ND-2000C

NanoDrop spectrophotometer (NanoDrop Technologies).

JunB protein purified *in vitro* was mixed with sodium chloride and DNA fragments (3×TRE or 7×TRE) at different concentrations. JunB protein was added to a flow cell and placed at 37℃ for 2 min. The sequences of 3×TRE are TGACTCATGACTCATGACTCA (5'-3') and TGAGTCATGAGTCATGAGTCA (3'-5'). The sequences of 7×TRE are TGACTCATGACTCATGACTCATGACTCATGACTCATGACTCATGACTCA (5'-3') and TGAGTCATGAGTCATGAGTCATGAGTCATGAGTCATGAGTCATGAGTCA (3'-5').

Sequence analysis for protein disorder

We used the PONDR program (http://www.disprot.org/index.php) to analyze disordered regions of JunB at default settings (Xue et al., 2010). Three predictors (VLXT, VL3, and VSL2B) indicated that JunB has a high disorder disposition.

Extraction of vascular ECs

C57BL/6 mice and db/db mice were purchased from Gempharmatech Company. After the neck was severed in C57BL/6 mice or db/db mice, the aorta was cut off from the heart link to the tip of the abdominal aorta with microscopic scissors and then placed on pre-cooled PBS. The connective tissue and fascia around the blood vessels were separated under a microscope. The vascular lumen was cut lengthwise, and the blood vessels were digested with type 2 collagenase (2 mg/ml) at 37℃ for 30 min. The digested cells were filtered with a 70-μm cell sieve and stained with CD31 (BD Biosciences), and the positive cells were sorted and collected by flow cytometry.

ChIP–qPCR

After cell adhesion culture, the number of cells was $\geq 1 \times 10^7$. Sample preparation was performed using a SimpleChIP Enzymatic Chromatin IP Kit. The protein and DNA were cross-linked and added into a 15-cm petri dish containing 20 ml medium with 540 μl of 37% formaldehyde until the final concentration was 1% and incubated at room temperature for 10 min (the cell density for suspended cells was $<0.5 \times 10^6$/ml). The crosslinking reaction was terminated by adding glycine (10×). Pre-cooled PBS was added to the petri dish (1% cooktail was added), the cells were scraped off, and nuclear preparation and chromatin digestion continued. The cells were suspended in 1 ml of 1×Buffer A (250 μl 4× Buffer A (#7006) plus 750 μl ddH_2O) and incubated on ice for 10 min. The cell suspension was centrifuged at 2000× *g*, 4℃ for 5 min, and the supernatant was removed and discarded. Then, 1.1 ml of 1×Buffer B (275 μl 4×Buffer B (#7007) plus 825 μl ddH_2O) was prepared, and cells were suspended in 1 ml of 1×Buffer B. After centrifugation, the supernatant was discarded and re-concentrated. After centrifugation, the supernatant was removed and re-suspended in 100 μl

of 1× Buffer B. The samples were transferred to a 1.5-ml centrifuge tube, and each sample was added with 0.5 μl Micrococcal Nuclease to digest the DNA fragments on ice for 20 min. After 10 μl 0.5 M EDTA was added to stop digestion, the cell membrane was broken by ultrasound with several pulses. Then, the samples were centrifuged at 9400× *g*, 4℃ for 10 min to clarify the dissolved matter. ChIP was performed by adding 400 μl of 1× ChIP Buffer (40 μl 10× ChIP Buffer (#7008) plus 360 μl ddH_2O) and 100 μl (5–10 μg) of chromatin to each sample. Meanwhile, the corresponding antibodies and IgG were added. Histone H3 (D2B12) XPs rabbit mAb (#4620) was used as a positive control group, and IgG (#2729) was used as a negative control group. The IP sample was incubated at 4℃ for 4 h. Then, 30 μl of ChIP protein G magnetic bead (#9006) was added to each IP reaction and incubated at 4℃ for 2 h. Each immunoprecipitation tube with protein G beads was placed in a magnetic separator for 1–2 min, and the superserum was carefully removed. The low-salt wash was repeated three times. Then, 1 ml of high-salt washing solution was added, and the mixture was rotate at 4℃ for 5 min. For elution of chromatin in antibody/protein G magnetism, 150 μl of 1× ChIP elution buffer was added to each IP sample and incubated at 65℃, 30 min by gently swirling the tube. The eluted chromatin supernatant was carefully transferred to a new tube by placing the tube on a magnetic separation rack to make granular protein G magnetic beads and waiting 1–2 min for the solution to be clear. All samples were added with 6 μl 5M NaCl and 2 μl protease K (#10012) and incubated at 65℃ for 2 h. DNA was purified using columns, and 50 μl DNA eluting buffer (#10009) was added to each rotating column and placed in a clean 1.5-ml centrifuge tube, followed by centrifugation at 18500× *g* for 30 sec to elute DNA. SimpleChIP Universal qPCR Master Mix was used for amplification.

Supplementary References

Xue, B., Dunbrack, R.L., Williams, R.W. et al. (2010). PONDR-FIT: a meta-predictor of intrinsically disordered amino acids. Biochim Biophys Acta 1804, 996-1010.

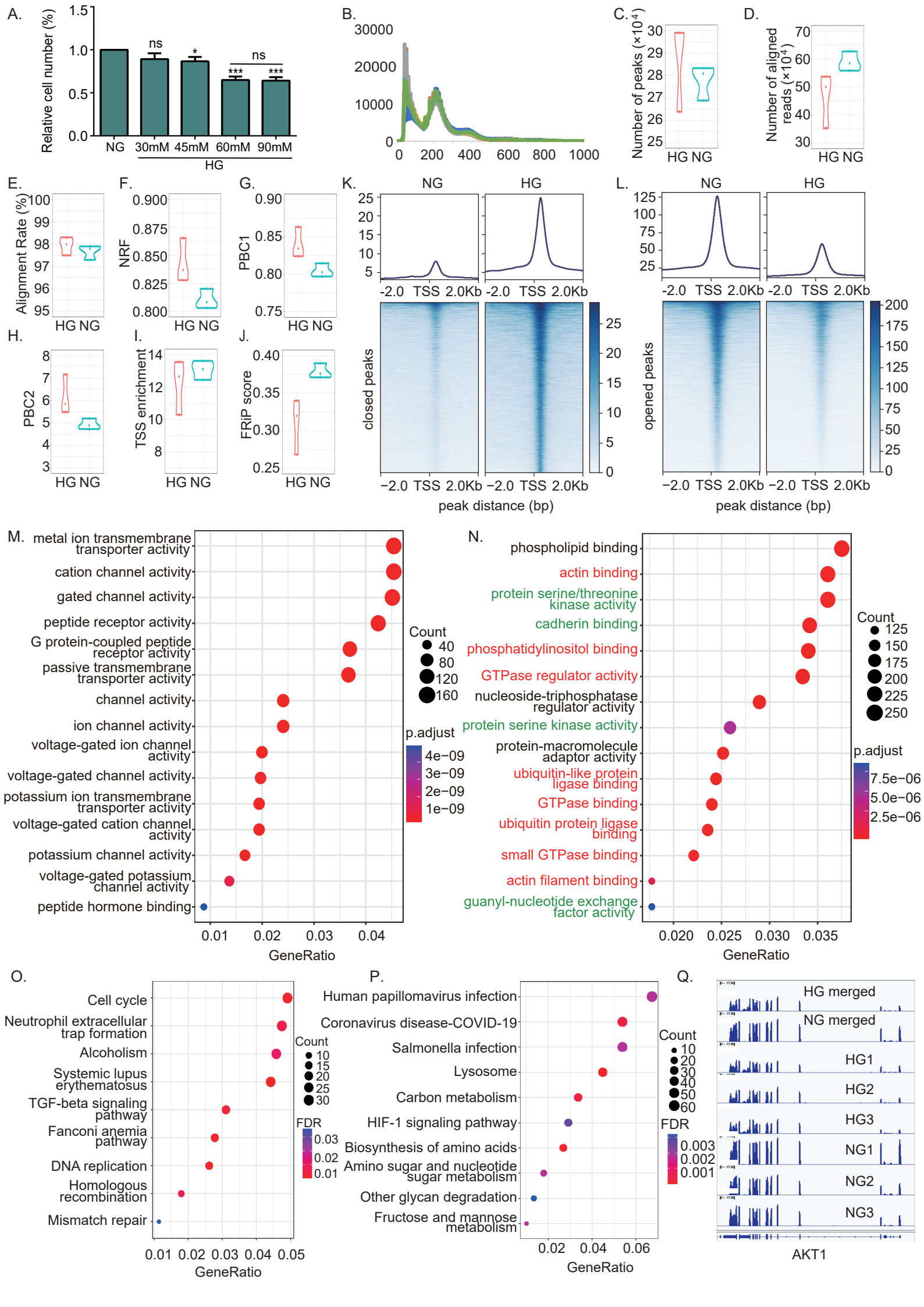
A.
Relative cell number (%)
1.5
1.0
0.5
0.0
ns
*
ns
***
***
NG
30mM
45mM
60mM
90mM
HG
B.
30000
20000
10000
0
0
200
400
600
800
1000
C.
Number of peaks (×10^4)
30
29
28
27
26
25
HG NG
D.
Number of aligned reads (×10^4)
70
60
50
40
30
HG NG
E.
Alignment Rate (%)
100
99
98
97
96
95
HG NG
F.
NRF
0.900
0.875
0.850
0.825
0.800
HG NG
G.
PBC1
0.90
0.85
0.80
0.75
HG NG
H.
PBC2
8
7
6
5
4
3
HG NG
I.
TSS enrichment
14
12
10
8
HG NG
J.
FRiP score
0.40
0.35
0.30
0.25
HG NG
K.
NG
HG
25
20
15
10
5
-2.0 TSS 2.0Kb
-2.0 TSS 2.0Kb
closed peaks
25
20
15
10
5
0
−2.0 TSS 2.0Kb
−2.0 TSS 2.0Kb
peak distance (bp)
L.
NG
HG
125
100
75
50
25
-2.0 TSS 2.0Kb
-2.0 TSS 2.0Kb
opened peaks
200
175
150
125
100
75
50
25
0
−2.0 TSS 2.0Kb
−2.0 TSS 2.0Kb
peak distance (bp)
M.
metal ion transmembrane transporter activity
cation channel activity
gated channel activity
peptide receptor activity
G protein-coupled peptide receptor activity
passive transmembrane transporter activity
channel activity
ion channel activity
voltage-gated ion channel activity
voltage-gated channel activity
potassium ion transmembrane transporter activity
voltage-gated cation channel activity
potassium channel activity
voltage-gated potassium channel activity
peptide hormone binding
0.01
0.02
0.03
0.04
GeneRatio
Count
40
80
120
160
p.adjust
4e−09
3e−09
2e−09
1e−09
N.
phospholipid binding
actin binding
protein serine/threonine kinase activity
cadherin binding
phosphatidylinositol binding
GTPase regulator activity
nucleoside-triphosphatase regulator activity
protein serine kinase activity
protein-macromolecule adaptor activity
ubiquitin-like protein ligase binding
GTPase binding
ubiquitin protein ligase binding
small GTPase binding
actin filament binding
guanyl-nucleotide exchange factor activity
0.020
0.025
0.030
0.035
GeneRatio
Count
125
150
175
200
225
250
p.adjust
7.5e−06
5.0e−06
2.5e−06
O.
Cell cycle
Neutrophil extracellular trap formation
Alcoholism
Systemic lupus erythematosus
TGF-beta signaling pathway
Fanconi anemia pathway
DNA replication
Homologous recombination
Mismatch repair
0.01
0.02
0.03
0.04
0.05
GeneRatio
Count
10
15
20
25
30
FDR
0.03
0.02
0.01
P.
Human papillomavirus infection
Coronavirus disease-COVID-19
Salmonella infection
Lysosome
Carbon metabolism
HIF-1 signaling pathway
Biosynthesis of amino acids
Amino sugar and nucleotide sugar metabolism
Other glycan degradation
Fructose and mannose metabolism
0.02
0.04
0.06
GeneRatio
Count
10
20
30
40
50
60
FDR
0.003
0.002
0.001
Q.
HG merged
NG merged
HG1
HG2
HG3
NG1
NG2
NG3
AKT1

Figure S1. JunB exhibits the reductions in both motif accessibility and gene expression level under high-glucose induction. Related to Figure 1.−

(A) The effects of high glucose with different concentrations on influencing HUVEC cell number.

(B) Fragment size distribution of ATAC-seq libraries obtained from each sample. Clear modulation of signals indicates nucleosome-free, mononucleosome and dinucleosome regions.

(C) The distribution of the number of peaks across all samples.

(D) The distribution of the number of reads after alignment and filtering across all samples.

(E) The distribution of the percentage of reads after alignment and filtering across all samples.

(F) The distribution of Non Redundant Fraction (NRF) across all samples.

(G) The distribution of PCR Bottlenecking Coefficients 1 (PBC1) across all samples.

(H) The distribution of PCR Bottlenecking Coefficients 2 (PBC2) across all samples.

(I) The distribution of the transcription start site (TSS) enrichment scores across all samples.

(J The distribution of the fraction of reads in called peak regions (FRiP) scores across all samples.

(K and L) Heatmaps showing chromatin accessibility in increased accessible (K) and decreased accessible (L) regions comparing HG to NG. For the heatmaps, ATAC counts of all 3 samples per group were merged. Plots on the top show the average ATAC-signal across regions.

(M and N) Gene ontology (GO) analysis of HG and NG was performed on the nearest genes of increased accessible (M) and decreased accessible (N) regions. Gene ratio refers to the ratio of the number of genes enriched in each term to the total number of genes in the term. Green, related to proliferation; Red, related to apoptosis.

(O and P) Kyoto Encyclopedia of Genes and Genomes (KEGG) analysis of HG and NG was performed on decreased expressed (O) and increased expressed (P) genes.

(Q) Genome browser tracks show mRNA-seq signals of AKT1 gene in all samples. All

the track lines have the same Y axis limits and that the peak height is normalized by the total read depth of each sample.

Error bars represent mean ± SD, n = 3 independent experiments if not stated. Significance was determined using two-tailed t test. * $P < 0.05$, ** $P < 0.01$, *** $P < 0.001$, **** $P < 0.0001$.

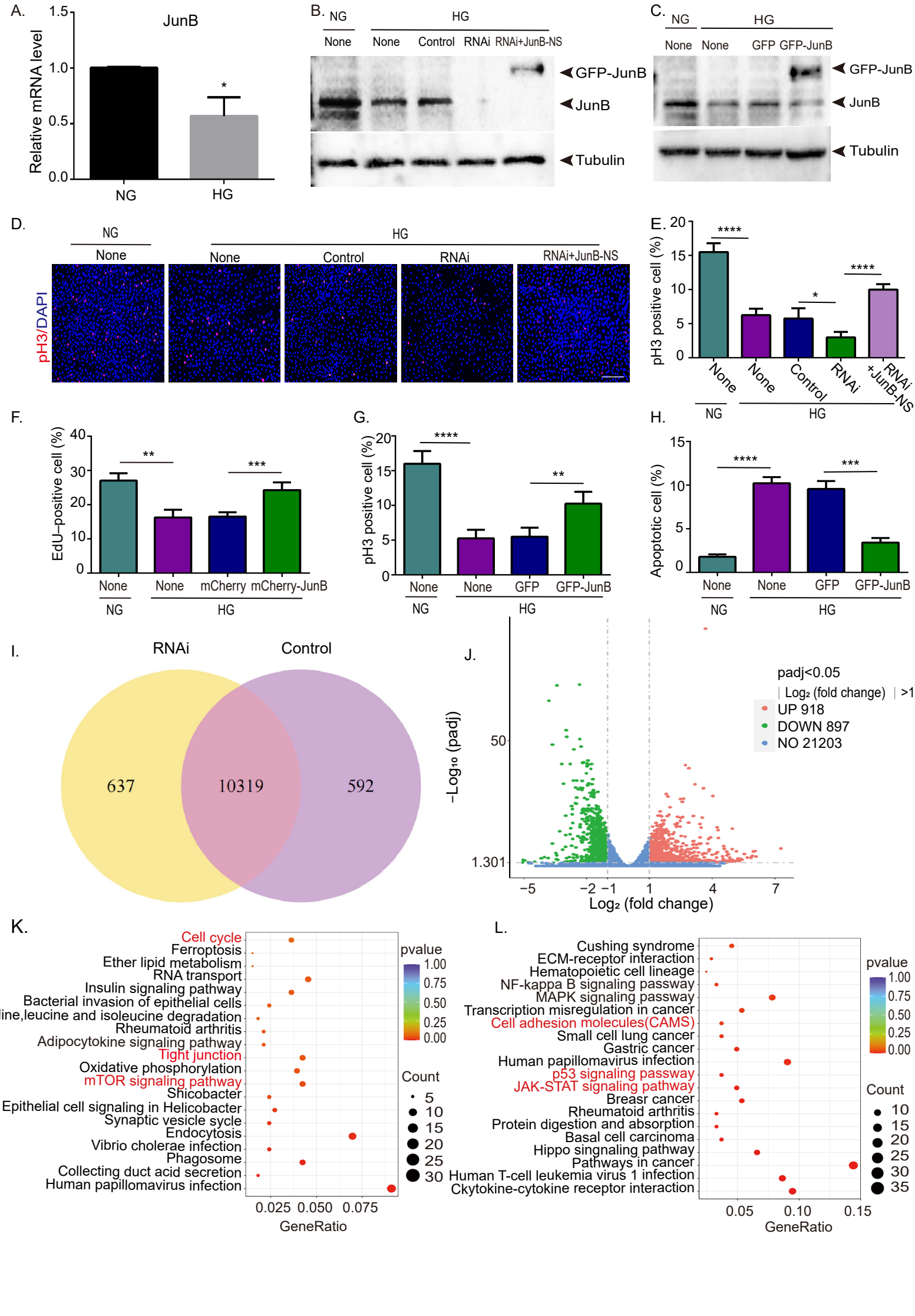
A.
JunB
Relative mRNA level
1.5
1.0
0.5
0.0
*
NG
HG
B.
NG
HG
None
None
Control
RNAi
RNAi+JunB-NS
GFP-JunB
JunB
Tubulin
C.
NG
HG
None
None
GFP
GFP-JunB
GFP-JunB
JunB
Tubulin
D.
NG
HG
None
None
Control
RNAi
RNAi+JunB-NS
pH3/DAPI
E.
pH3 positive cell (%)
20
15
10
5
0
****
*
****
None
None
Control
RNAi
RNAi +JunB-NS
NG
HG
F.
EdU–positive cell (%)
40
30
20
10
0
**
***
None
None
mCherry
mCherry-JunB
NG
HG
G.
pH3 positive cell (%)
20
15
10
5
0
****
**
None
None
GFP
GFP-JunB
NG
HG
H.
Apoptotic cell (%)
15
10
5
0
****
***
None
None
GFP
GFP-JunB
NG
HG
I.
RNAi
Control
637
10319
592
J.
padj<0.05
Log₂ (fold change) >1
UP 918
DOWN 897
NO 21203
−Log₁₀ (padj)
50
1.301
−5
−2
−1
1
4
7
Log₂ (fold change)
K.
Cell cycle
Ferroptosis
Ether lipid metabolism
RNA transport
Insulin signaling pathway
Bacterial invasion of epithelial cells
Valine,leucine and isoleucine degradation
Rheumatoid arthritis
Adipocytokine signaling pathway
Tight junction
Oxidative phosphorylation
mTOR signaling pathway
Shicobacter
Epithelial cell signaling in Helicobacter
Synaptic vesicle sycle
Endocytosis
Vibrio cholerae infection
Phagosome
Collecting duct acid secretion
Human papillomavirus infection
pvalue
1.00
0.75
0.50
0.25
0.00
Count
5
10
15
20
25
30
0.025
0.050
0.075
GeneRatio
L.
Cushing syndrome
ECM-receptor interaction
Hematopoietic cell lineage
NF-kappa B signaling passway
MAPK signaling passway
Transcription misregulation in cancer
Cell adhesion molecules(CAMS)
Small cell lung cancer
Gastric cancer
Human papillomavirus infection
p53 signaling passway
JAK-STAT signaling pathway
Breasr cancer
Rheumatoid arthritis
Protein digestion and absorption
Basal cell carcinoma
Hippo singnaling pathway
Pathways in cancer
Human T-cell leukemia virus 1 infection
Ckytokine-cytokine receptor interaction
pvalue
1.00
0.75
0.50
0.25
0.00
Count
10
15
20
25
30
35
0.05
0.10
0.15
GeneRatio

Figure S2. JunB reversed the effects of high glucose on endothelial cell proliferation and apoptosis. Related to Figure 2.

(A-H) Effects of 60mM glucose treatment on the JunB level, proliferation and apoptosis of HUVECs.

(A) RT-qPCR of HUVECs treated with high glucose showed the increased mRNA level of JunB.

(B) Western blotting showed high glucose and RNAi reduced the protein level of JunB, and rescue increased the protein level of JunB-NS.

(C) Western blotting showed high glucose reduced the protein level of JunB, and overexpression by lentivirus infection increased the protein level of GFP-JunB.

(D and E) The cell proliferation of JunB RNAi and rescue HUVECs treated with high glucose was determined by pH3 assay. Representative images of pH3 and DAPI staining (D) and the percentage of pH3 positive cell (E). Scale bar, 250 μm.

(F) The cell proliferation of mCherry-JunB overexpression HUVECs treated with high glucose was determined by EdU assay, and the percentage of EdU-positive cell were shown.

(G) The cell proliferation of GFP-JunB overexpression HUVECs treated with high glucose was determined by pH3 assay, and the percentage of pH3 positive cell were shown.

(H) Detect apoptotic cells of GFP-JunB overexpression HUVECs treated with high glucose by flow cytometry, and the percentage of apoptotic cell were shown.

(I) Venn diagram between the genes expressed in the HUVECs treated with control (purple circle) and JunB RNAi (orange circle) under the high-glucose induction.

(J) Volcano plot of RNA-seq genes comparing control and JunB RNAi HUVECs treated with high glucose. Genes with differentially expressed (padj < 0.05 and $|\log_2(\text{Fold Change})| > 1$) are highlighted. The number of genes with increased (red) and decreased (green) expression were calculated.

(K and L) Kyoto Encyclopedia of Genes and Genomes (KEGG) analysis of control and JunB RNAi HUVECs treated with high glucose was performed on decreased expressed (K) and increased expressed (L) genes ranked by the $\log_2$(Fold Change) using the R

package "clusterProfiler". Gene ratio refers to the ratio of the number of genes enriched in each term to the total number of genes in the term.

Error bars represent mean ± SD, n = 3 independent experiments if not stated. Significance was determined using two-tailed t test. * $P < 0.05$, ** $P < 0.01$, *** $P < 0.001$, **** $P < 0.0001$.

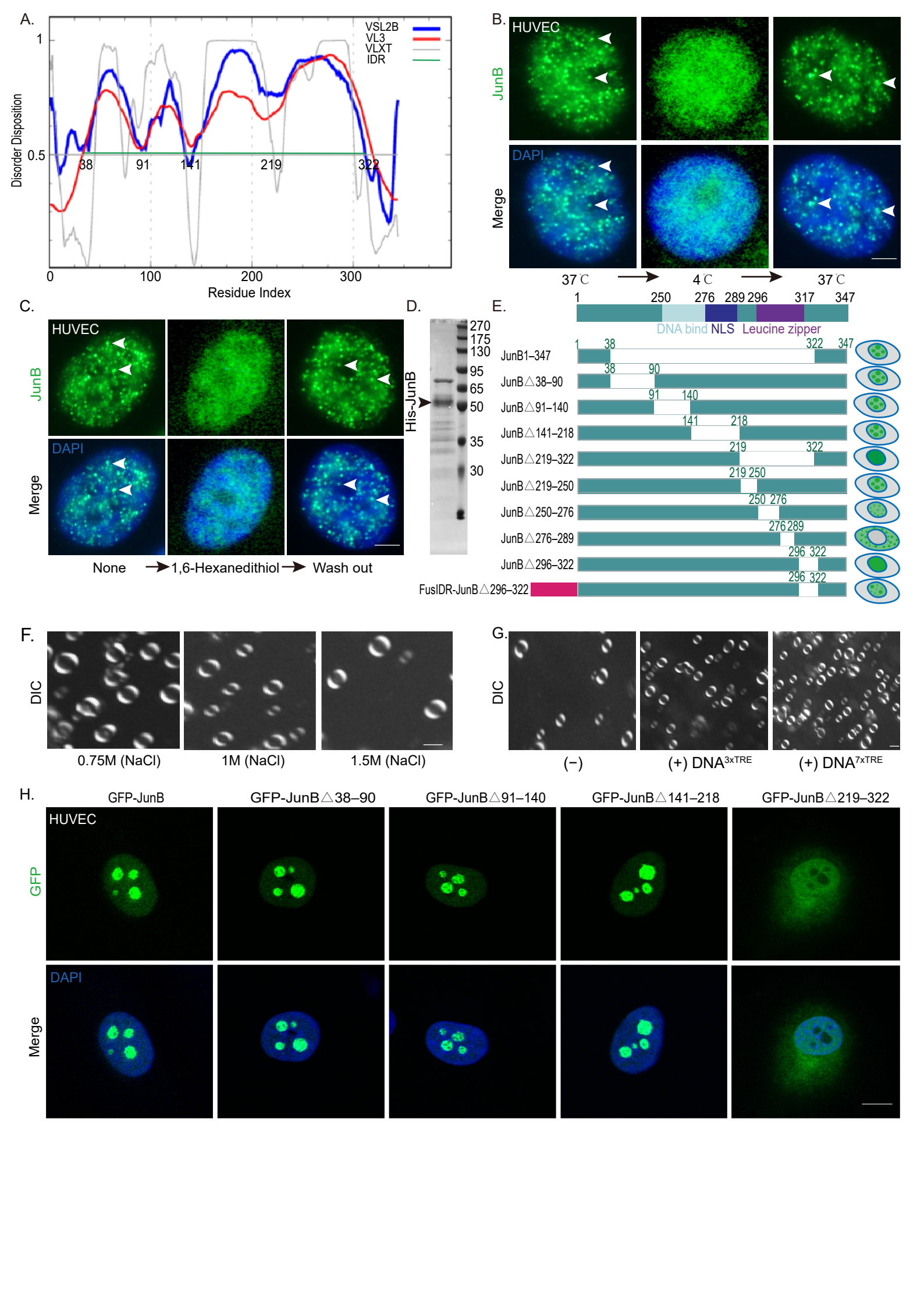
A.
VSL2B
VL3
VLXT
IDR
Disorder Disposition
1
0.5
38
91
141
219
322
0
100
200
300
Residue Index
B.
HUVEC
JunB
DAPI
Merge
37 ℃
4 ℃
37 ℃
C.
HUVEC
JunB
DAPI
Merge
None
1,6-Hexanedithiol
Wash out
D.
His-JunB
270
175
130
95
65
50
35
30
E.
1
250
276
289
296
317
347
DNA bind
NLS
Leucine zipper
JunB1–347
JunB△38–90
JunB△91–140
JunB△141–218
JunB△219–322
JunB△219–250
JunB△250–276
JunB△276–289
JunB△296–322
FusIDR-JunB△296–322
F.
DIC
0.75M (NaCl)
1M (NaCl)
1.5M (NaCl)
G.
DIC
(−)
(+) DNA3xTRE
(+) DNA7xTRE
H.
GFP-JunB
GFP-JunB△38–90
GFP-JunB△91–140
GFP-JunB△141–218
GFP-JunB△219–322
HUVEC
GFP
DAPI
Merge

Figure S3. In nucleus and in vitro, JunB undergoes LLPS. Related to Figure 3.

(A) Sequence features of JunB. The line at 0.5 (y axis) is the cutoff for disorder (> 0.5) and order (< 0.5) predictions. VSL2B, VL3, and VLXT, predictors for disordered dispositions. IDR, predicted internal disorder region.

(B) Temperature-dependent puncta diffusion and re-formation of JunB in the nuclei of HUVECs by immunofluorescence staining. Temperature ramp, 4℃-37℃. Scale bar, 5 μm.

(C) The incubated and wash-out of 1,6-hexanediol led puncta dissolution and re-formation of JunB in the nuclei of HUVECs by immunofluorescence staining. Scale bar, 5 μm.

(D) Coomassie brilliant blue staining of JunB protein purified in vitro. The arrow showed His-JunB.

(E) Illustration depicting how different mutants of JunB were constructed.

(F) The NaCl concentration varying among 0.75M, 1M, 1.5M modulated the formation of JunB droplets in vitro. Scale bar, 2 μm.

(G) The concentration of DNA fragment TRE repeat varying among 0, 3xTRE and 7xTRE modulated the formation of JunB droplets in vitro. Scale bar, 2 μm.

(H) Different GFP-JunB mutants were overexpressed in HUVECs to observe the formation of puncta. Scale bar, 10 μm.

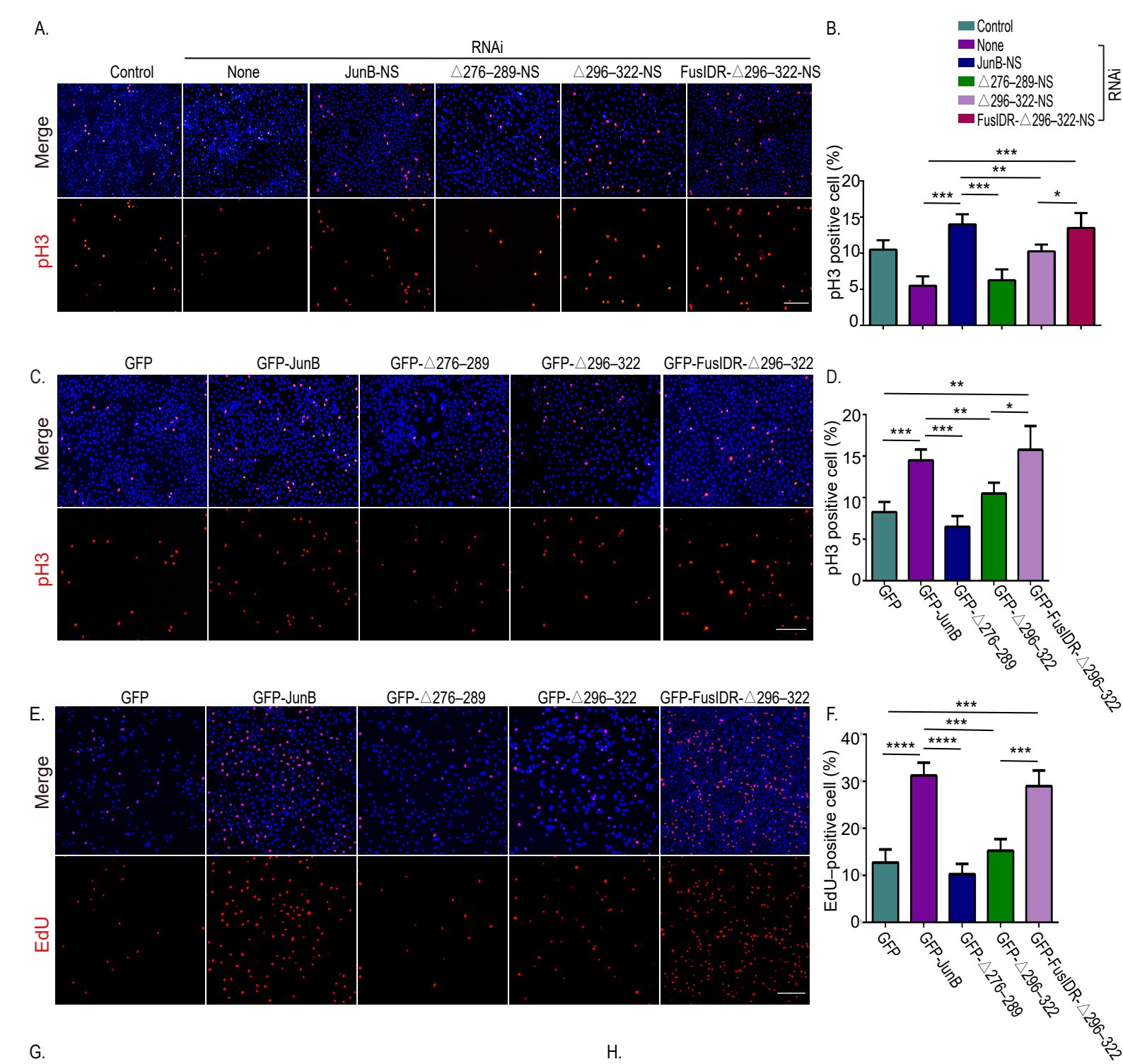
A.
RNAi
Control
None
JunB-NS
△276–289-NS
△296–322-NS
FusIDR-△296–322-NS
Merge
pH3
B.
Control
None
JunB-NS
△276–289-NS
△296–322-NS
FusIDR-△296–322-NS
RNAi
pH3 positive cell (%)
C.
GFP
GFP-JunB
GFP-△276–289
GFP-△296–322
GFP-FusIDR-△296–322
Merge
pH3
D.
pH3 positive cell (%)
E.
GFP
GFP-JunB
GFP-△276–289
GFP-△296–322
GFP-FusIDR-△296–322
Merge
EdU
F.
EdU–positive cell (%)
G.
GFP IP
GFP-JunB (NG)
GFP-JunB (HG)
GFP-△296–322 (HG)
GFP-FusIDR-△296–322 (HG)
Fold enrichment
VEGFB
Ywhab
H.
JunB IP
Wild type mice
db/db mice
Fold enrichment
VEGFB
Ywhab

Figure S4. The nuclear localization and condensation of JunB modulate its functions in endothelial cell proliferation and apoptosis induced by high glucose. Related to Figure 4.

(A-B) The cell proliferation of JunB RNAi HUVECs treated with high glucose, lentivirus infection with different mutants after JunB RNAi,and overexpression of different JunB-NS mutants by lentivirus infection was determined by pH3 assay. Representative images of pH3 and DAPI staining (A) and the percentage of pH3 positive cell (B). Scale bar, 250 μm.

(C-D) The cell proliferation of HUVECs treated with high glucose and overexpressed by different GFP-JunB mutants was determined by pH3 assay. Representative images of pH3 and DAPI staining (C) and the percentage of pH3 positive cell (D). Scale bar, 250 μm.

(E-F) The cell proliferation of HUVECs treated with high glucose and overexpression of different GFP-JunB mutants by lentivirus infection was determined by EdU incorporation assay. Representative images of EdU incorporation and DAPI staining (E) and the percentage of EdU-positive cell (F). Scale bar, 250 μm.

(G) Results of ChIP-qPCR assays in HUVECs under different treatments and conditions.

(H) Results of ChIP-qPCR assays with vascular endothelial cells isolated from C57BL/6 mice or db/db mice

Error bars represent mean ± SD, n = 3 independent experiments if not stated.

Significance was determined using two-tailed t test. * $P < 0.05$, ** $P < 0.01$, *** $P < 0.001$.

Table S1. Primers for different plasmid constructs in this study

Name	Forward primer (5'-3')	Reverse primer (3'-5')
pET-32a-His-JunB	AAGGCCATGGCTGATATCGGATCCATGTGCACTAAAATGGAACAGC	ACGGAGCTCGAATTCGGATCCTCAGAAGGCGTGTCCCT
PLV-GFP-JUNB	TCAGATCTCGAGCTCAAGCTTCGATGTGCACTAAAATGGAACAGC	CGGTACCGTCGACTGCAGATCAGAAGGCGTGTCCCT
PLV-mCherry-JUNB	TCAGATCTCGAGCTCAAGCTTCGATGTGCACTAAAATGGAACAGC	CGGTACCGTCGACTGCAGATCAGAAGGCGTGTCCCT
PLV-JUNB-NS	CTACTCAAGCCGAGCCTGGCGGTCAACCT	CTTATAATCGTGTAGAGAGAGGCCACCAGGGGCCC
PLV-JUNBΔ 37-90	ATTGTCCCCAACAGCAACGGC	CGGTTTCAGGAGTTTGTAGTCGTGTAGAGA
PLV-JUNBΔ 91-140	AAAGCCCTGGACGATCTGCAC	CAGGCGTTCCAGCTCCGAA
PLV-JUNBΔ 141-218	GCGCCGCCCTTCGCC	GACAAAGCCGTCGGCGAAGC
PLV-JUNBΔ 219-322	CAGCTCAAACAGAAGGTCATGACCCAC	GTGTGGGAGGTAGCTGATGGTGG
PLV-JUNBΔ 219-250	AGCCGGGACGCCACG	GTGTGGGAGGTAGCTGATGGTGG
PLV-JUNBΔ 250-276	CGGAACCGGCTGGCGG	CGCCTCCGGCACGGT
PLV-JUNBΔ 276-289	CTGGAGCGCATCGCGC	CCGCTTGCGCTCCACTTTGA
PLV-JUNBΔ 296-322	CAGCTCAAACAGAAGGTCATGACCCAC	GCGCGCGATGCGCT
PLV-FusIDR-JUNBΔ296-322	TCAGATCTCGAGCTCAAGCTTCGATGGCCTCAAACGATTATACCC	TCAGATCTCGAGCTCAAGCTTCGATGGCCTCAAACGATTATACCC

Name	**Forward primer (5'-3')**	**Reverse primer (3'-5')**
PLV-JUNBΔ 37-90-NS	ATTGTCCCCAACAGCAACGGC	CGGTTTCAGGAGTTTGTAGTCGTGTAGAGA
PLV-JUNBΔ 91-140-NS	AAAGCCCTGGACGATCTGCAC	CAGGCGTTCCAGCTCCGAA
PLV-JUNBΔ 141-218-NS	GCGCCGCCCTTCGCC	GACAAAGCCGTCGGCGAAGC
PLV-JUNBΔ 219-322-NS	CAGCTCAAACAGAAGGTCATGACCCAC	GTGTGGGAGGTAGCTGATGGTGG
PLV-JUNBΔ 219-250-NS	AGCCGGGACGCCACG	GTGTGGGAGGTAGCTGATGGTGG
PLV-JUNBΔ 250-276-NS	CGGAACCGGCTGGCGG	CGCCTCCGGCACGGT
PLV-JUNBΔ 276-289-NS	CTGGAGCGCATCGCGC	CCGCTTGCGCTCCACTTTGA
PLV-JUNBΔ 296-322-NS	CAGCTCAAACAGAAGGTCATGACCCAC	GCGCGCGATGCGCT
PLV-FusIDR-JUNBΔ296-322-NS	TCAGATCTCGAGCTCAAGCTTCGATGGCCTCAAACGATTATACCC	TCAGATCTCGAGCTCAAGCTTCGATGGCCTCAAACGATTATACCC

Table S2. Primers for RT-qPCR in this study

Gene name	Forward primer (5'-3')	Reverse primer (3'-5')
JunB	AACAGCCCTTCTACCACGAC	CAGGCTCGGTTTCAGGAGTT
CDC25B	GCATGGAGAGTCTCATTAGTGC	CTCCGCCTCCGCTTATTCT
SKP1	AAGACCATGTTGGAAGATTTGGGA	ATCTTCAGGAGGAGGAGGGTC
YWHAB	CTGGAGACAACAAACAAACCACT	GAATTGGGTGTGTAGGCTGC
MAD2L1	GGCCGAGTTCTTCTCATTCG	TTACAAGCAAGGTGAGTCCGT
GADD45A	GAGAGCAGAAGACCGAAAGGA	CACAACACCACGTTATCGGG
GADD45B	TACGAGTCGGCCAAGTTGATG	GGATGAGCGTGAAGTGGATTT
BBC3	GCCAGATTTGTGAGACAAGAGG	CAGGCACCTAATTGGGCTC
actin	TGTCACCAACTGGGACGATA	GGGGTGTTGAAGGTCTCAAA
VEGFB-human (ChIP)	ACTGCTAGCAGCCTGC	AGGGCTCAGAGTGGC
VEGFB-mouse (ChIP)	TGCCTCCAGAAAGCTCCAGG	CCTGGAGGCCGAGCTCC
Ywhab-human (ChIP)	AGACAGGGTCTCACTCTGTCTC	GTAGGGTCGAGCAGTG
Ywhab-mouse (ChIP)	GCTGAGCAAGGCAGCATCTC	GGTTTCTATTGCTGTGATGCTGGG

Table S3. Reagent used in this study

Reagent	Source	Identifier
Antibodies		
anti-JunB	Abcam	Cat# ab128878
anti-JunB	Cell Signaling Technology	Cat# 3753S
anti-pH3	Millipore	Cat# 06-570
anti-CD31	BD Biosciences	Cat#561073
anti-Tubulin	Cell Signaling Technology	Cat#2148S; RRID:AB_2288042
Goat anti-Rabbit IgG (H+L) Highly Cross-Adsorbed Secondary Antibody, Alexa Fluor™ 488	Thermo Fisher Scientific	Cat# A-11001; RRID: AB_2534069
Goat anti-Rabbit IgG (H+L) Highly Cross-Adsorbed Secondary Antibody, Alexa Fluor™ 647	Thermo Fisher Scientific	Cat# A-21235; RRID: AB_2535804
goat anti-rabbit HRP	Beyotime Biotechnology	Cat# A0208; RRID:AB_2892644
Chemicals, peptides, and recombinant proteins		
DMEM medium	Gibco	Cat# C11885500cp
fetal bovine serum	Gibco	Cat# 16000-044
1,6-hexanediol	sigma	Cat#240117
polyBrene	Solarbio	Cat# H8761
DAPI (4’,6-Diamidino-2-phenylindole dihydrochloride)	Sigma-Aldrich	Cat# D8417
Trypsin-EDTA	Thermo Fisher Scientific	Cat# 15400-054
Triton X-100	Biofroxx	Cat# 9002-93-1

Reagent	**Source**	**Identifier**
Critical commercial assays		
HiScript III RT SuperMix for qPCR	Vazyme	Cat# R323-01
SimpleChIP Enzymatic Chromatin IP Kit	Cell Signaling Technology	Cat# 91820
SimpleChIP Universal qPCR Master Mix	Cell Signaling Technology	Cat# 88989P
ChromoTek GFP-Trap® Magnetic Agarose	proteintech	Cat# gtma
lipofectamine RNAiMAX	Invitrogen	Cat# 13778150
MinElute PCR Purification Kit	Qiagen	Cat# 28004
Collagenase II	Worthington	Cat# LS004176
Q5 Site-Directed Mutagenesis Kit	NEB	Cat#E0552S
QuickBlock™ Blocking Buffer for Western Blot	Beyotime	Cat# P0256
TruePrepTM DNA Library Prep Kit V2 for Illumina®	Vazyme	Cat# TD501-02
TUNEL BrightRed Apoptosis Detection Kit	Vazyme	Cat# A113-01
DeadEnd™ Fluorometric TUNEL System	Promega	Cat#G328A
VAHTS DNA Clean Beads	Vazyme	Cat# N411
Lipo8000™ Transfection Reagent	Beyotime Biotechnology	Cat# C0533
BCA kit	BOSTER	Cat# AR0146A
ChamQ Universal SYBR qPCR Master Mix	Vazyme	Cat# Q711-02
ECL Prime Western Blotting Detection Reagent	Thermo	Cat# 45-002-401
EDU Kit	Abbkine	Cat#KTA2030

Reagent	**Source**	**Identifier**
EDU Kit	Abbkine	Cat#KTA2031
Deposited data		
RNA-sequencing data	This paper	N/A
ATAC-seq data	This paper	N/A
Experimental models: Cell lines		
293T cell	ATCC	N/A
HUVEC	ATCC	N/A
Software and algorithms		
Prism 7.0	GraphPad	https://www.graphpad.
LAS X	Leica	N/A